# *In vivo* mouse inferior olive neurons exhibit heterogeneous subthreshold oscillations and spiking patterns

S. Khosrovani*, R. S. Van Der Giessen*, C. I. De Zeeuw*†‡, and M. T. G. De Jeu*

*Department of Neuroscience, Erasmus University Medical Center, P.O. Box 2040, 3000 CA, Rotterdam, The Netherlands; and †Netherlands Institute for Neuroscience, Royal Academy of Sciences (KNAW), 1105 BA, Amsterdam, The Netherlands

Edited by Rodolfo R. Llinas, New York University Medical Center, New York, NY, and approved August 22, 2007 (received for review March 30, 2007)

***In vitro*** **whole-cell recordings of the inferior olive have demonstrated that its neurons are electrotonically coupled and have a tendency to oscillate. However, it remains to be shown to what extent subthreshold oscillations do indeed occur in the inferior olive *in vivo* and whether its spatiotemporal firing pattern may be dynamically generated by including or excluding different types of oscillatory neurons. Here, we did whole-cell recordings of olivary neurons *in vivo* to investigate the relation between their subthreshold activities and their spiking behavior in an intact brain. The vast majority of neurons (85%) showed subthreshold oscillatory activities. The frequencies of these subthreshold oscillations were used to distinguish four main olivary subtypes by statistical means. Type I showed both sinusoidal subthreshold oscillations (SSTOs) and low-threshold $Ca^{2+}$ oscillations (LTOs) (16%); type II showed only sinusoidal subthreshold oscillations (13%); type III showed only low-threshold $Ca^{2+}$ oscillations (56%); and type IV did not reveal any subthreshold oscillations (15%). These subthreshold oscillation frequencies were strongly correlated with the frequencies of preferred spiking. The frequency characteristics of the subthreshold oscillations and spiking behavior of virtually all olivary neurons were stable throughout the recordings. However, the occurrence of spontaneous or evoked action potentials modified the subthreshold oscillation by resetting the phase of its peak toward 90°. Together, these findings indicate that the inferior olive in intact mammals offers a rich repertoire of different neurons with relatively stable frequency settings, which can be used to generate and reset temporal firing patterns in a dynamically coupled ensemble.**

membrane properties | motor coordination | olivocerebellar system | peripheral stimulation | rhythmicity

The inferior olive (IO) forms the sole source of the climbing fiber input to Purkinje cells in the cerebellar cortex (1). Single climbing fibers excite Purkinje cells in the cerebellar cortex, resulting in a powerful, all-or-none depolarization called the complex spike. *In vitro* studies have shown that olivary neurons have a unique combination of cellular properties, including electrotonic coupling and a propensity to oscillate (2–5). Their tendency to oscillate is mainly due to specific $Ca^{2+}$ conductances, which are distributed differentially over their membrane compartments (2, 6). Dendritic high-threshold and somatic low-threshold $Ca^{2+}$ conductances can activate each other rhythmically, and they can interact with a $Ca^{2+}$-dependent $K^+$ conductance, resulting in the production of subthreshold oscillations with amplitudes of 3–10 mV (2). To date, it is unknown to what extent these oscillations also occur *in vivo* and how they influence the generation of patterns of complex spike activities in the intact olivocerebellar system (see also ref. 7).

In the intact system, olivary neurons are integrated in specific cerebellar modules (1, 8, 9). The climbing fibers of each olivary subnucleus innervate the Purkinje cells of a particular zone, which in turn project back to the same olivary subnucleus via one of the cerebellar nuclei. In this way, the olivocerebellar system comprises many modules, which are each dedicated to specific motor domains and which can run in parallel if needed. The GABAergic feedback from the cerebellar nuclei to the IO is peculiar in that its fibers terminate in a strategic position inside glomeruli directly apposed to the olivary dendrites that are coupled by gap junctions (10). By inducing a large shunting current these terminals may be able to dynamically uncouple olivary neurons and thereby influence the synchrony of complex spike activities that occur in the cerebellar cortex (11–13). Such a mechanism may for example be involved during the training and execution of rhythmic, tongue or whisker movements (14, 15).

If the IO is indeed involved in setting the pace and composition of motor domains by controlling the activities of ensembles of coupled neurons then the question remains how the preferred frequency of an oscillating ensemble is determined. In principle, there are two main options for controlling such a frequency (1). Either olivary neurons are uniformly flexible and the preferred frequency of their oscillation can be controlled by activation of their excitatory afferents (in this constellation, inhibitory input from the cerebellar nuclei could serve to merely control the size of the coupled ensemble) or, alternatively, individual olivary neurons have a more unique, but fixed, preferred frequency of oscillation, and the preferred frequency of the ensemble is determined by including or excluding particular cells via their cerebellar GABAergic input. In the latter case, one should find different categories of olivary neurons with different, but fixed, preferred frequencies and one should not be able to change this frequency by peripheral activation.

Thus, to investigate the occurrence and stability of subthreshold oscillations of olivary neurons *in vivo*, to find out how they may influence the temporal pattern of their climbing fiber activities, and to study the impact of peripheral stimulation on these oscillations and spiking patterns, we performed whole-cell recordings of olivary neurons in the intact olivocerebellar system during peripheral sensory stimulation.

## Results

**Basic Membrane Properties.** Results described in this study were obtained from 61 neurons of the IO (i.e., principal olive, accessory olives, and dorsal cap of Kooy) measured by *in vivo* whole-cell recording technique. The basic membrane properties measured *in vivo* were comparable with those measured *in vitro* (2, 16–18) [supporting information (SI) Table 1]. The *in vivo* recorded IO

Author contributions: S.K. and R.S.V.D.G. contributed equally to this work; C.I.D.Z. and M.T.G.D.J. designed research; S.K. and R.S.V.D.G. performed research; S.K., R.S.V.D.G., and M.T.G.D.J. analyzed data; and S.K., R.S.V.D.G., C.I.D.Z., and M.T.G.D.J. wrote the paper.

The authors declare no conflict of interest.

This article is a PNAS Direct Submission.

Abbreviations: IO, inferior olive; SSTO; sinusoidal subthreshold oscillation; LTO, low-threshold $Ca^{2+}$ oscillation; ISI, interspike interval; EPSP, excitatory postsynaptic potential.

‡To whom correspondence should be addressed at: Department of Neuroscience, Erasmus Medical Center, Dr. Molewaterplein 60, 3000 DR, Rotterdam, The Netherlands. E-mail: c.dezeeuw@erasmusmc.nl.

This article contains supporting information online at www.pnas.org/cgi/content/full/0702727104/DC1.

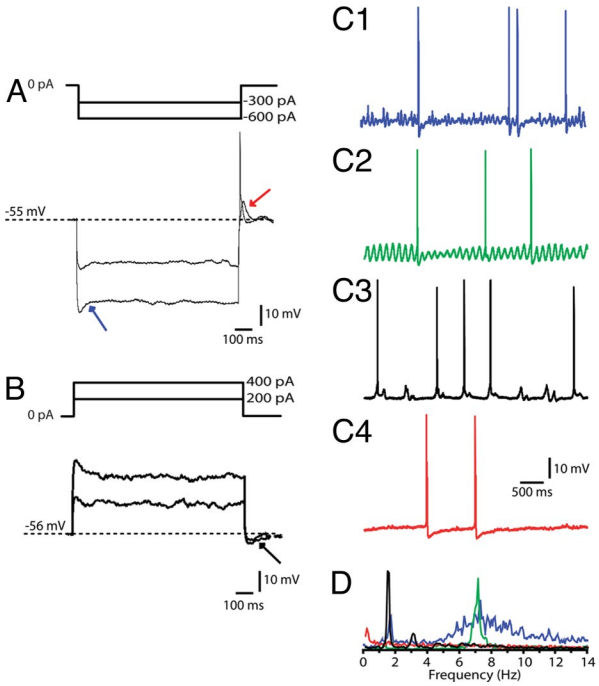


**Fig. 1.** Membrane properties of olivary neurons recorded in current clamp mode. (*A*) Hyperpolarizing current injections of 1 s were applied to evoke the time-dependent inward rectification ($I_H$; blue arrow) and rebound depolarizations (red arrow) as well as rebound spikes. It should be noted that type I and II neurons, which express a rebound depolarization, can initiate sinusoidal oscillations in response to this rebound depolarization. (*B*) Depolarizing current injections of 1 s were applied to induce an after hyperpolarization (AHP; black arrow). (*C*) Different types of subthreshold activity in the membrane potential were observed in olivary neurons. (*C1*) Neuron showing a subthreshold activity composed of two different frequencies, namely 1.9 Hz and 7.2 Hz. (*C2*) Neuron showing sine-wave shaped oscillations of 7 Hz. (*C3*) Cell with low-threshold $Ca^{2+}$ spikes, which exhibited a rhythmic behavior of 1.8 Hz. (*C4*) Cells without any substantial subthreshold activity. (*D*) Power spectra of the recordings shown in *C1*, *C2*, *C3*, and *C4*.

neurons fired action potentials with an average frequency of 0.87 ± 0.22 Hz and a mean regularity of 0.74 ± 0.02 [coefficient of variation (CV) of spike intervals]. They had a resting membrane potential of –55.6 ± 0.7 mV, a membrane capacitance of 184.0 ± 11.3 pF, and an input resistance of 45.9 ± 4.2 MΩ. Electrophysiological behavior of IO neurons was further studied by injection of positive and negative current pulses (Fig. 1 *A* and *B*). In contrast to previous *in vitro* studies, which often revealed a strong "depolarizing sag" as a result of activating H-currents (19, 20), our *in vivo* study showed a depolarizing sag in only a minority of the cases (18%; Fig. 1*A*). Moreover, the same negative current injection evoked a strong rebound depolarization in a majority of the cases (61%). Increasing the amplitude of negative current resulted in an increase of rebound depolarization and eventually a somatic low-threshold $Ca^{2+}$ spike was induced (Fig. 1*A*), which in turn triggered a fast sodium spike. Intracellular depolarizing current pulses hardly initiated action potentials or spike-adaptation and depolarizing steps were followed by a hyperpolarizing sag in only 23% of the cells (Fig. 1*B*).

Whole-cell recordings of IO neurons *in vivo* exhibited various patterns of resting membrane potential activity (Fig. 1*C*). In contrast to *in vitro* studies in which subthreshold sine-wave-shaped oscillations and rhythmic low-threshold $Ca^{2+}$ spikes virtually only occur in hyperpolarized neurons and in which they rarely occur together in the same neuron (2, 6), our *in vivo* recordings revealed that IO neurons can also exhibit these two types of oscillations spontaneously and relatively frequently together. We observed four different types of patterns of subthreshold activities: (*i*) typical rhythmic 4- to 8-Hz sinusoidal subthreshold oscillations (SSTOs) with a mean amplitude of 5.6 ± 0.6 mV (Fig. 1*C2*); (*ii*) rhythmic 1- to 3-Hz low-threshold $Ca^{2+}$ oscillations (LTOs) with a mean amplitude of 4.2 ± 0.3 mV (Fig. 1*C3*); (*iii*) a pattern in which both oscillatory activities described above were combined (Fig. 1*C1*); and (*iv*) a pattern in which no subthreshold oscillations were present in the resting membrane potential (Fig. 1*C4*). In the first three patterns, the amplitude of the oscillations could either be constant or vary in a cyclic manner. In the fourth pattern, there was a subpopulation (only three neurons) in which no low-threshold $Ca^{2+}$ currents were observed and in which the high firing frequencies (up to 30 Hz) could be evoked by depolarizations.

**Categorization of Neurons.** Because the patterns of subthreshold membrane activities seemed to vary considerably among IO neurons, we investigated whether the differences described above could be established by statistical means. Using the frequency of the subthreshold membrane oscillations as a distinguishing property in a hierarchical cluster analysis, we were indeed able to readily divide the population of 61 olivary neurons into four clusters (Fig. 2*A*): 16% of the neurons exhibited both SSTOs and LTOs (type I); 13% exhibited only SSTOs (type II); 56% contained neurons that exhibited only LTOs (type III); and 15% did not show any subthreshold oscillation (type IV). Moreover, the identity of these clusters could be readily confirmed in a matrix in which the LTO and SSTO activities were plotted against each other in the order of their frequencies (Fig. 2*B*). Despite their clear characteristics at the cell physiological level, type I, II, and III neurons that were intracellularly injected with neurobiotin were indistinguishable from each other at the morphological level (for all $n = 4$; SI Fig. 7*A*); they all showed the characteristic olivary dendrites that tend to curl back toward the soma (1) and they were not restricted to any particular olivary subnucleus (Fig. 2*C*). Because of their low occurrence, type IV neurons were not labeled, but three of these neurons were recorded in the medial part of the IO at a depth ranging from 500 to 750 μm and their activity closely resembles that of the neurons that were described by Urbano *et al.* (21). Therefore, these neurons are probably olivary neurons from the dorsal cap of Kooy.

To determine whether the identity of an individual olivary neuron is fixed, we investigated the stability of their subthreshold oscillations over time (on average 23 min). Two minutes of spontaneous recordings were compared with the same episodes of recordings at least 5–10 min later. Within the two minutes timeframes themselves no transitions in subthreshold activities were observed (Fig. 3*A*). However, 4 of the 61 neurons (7%) showed a change in one of the subsequent episodes with respect to the first one (Fig. 3*B*). Two type I cells became type III cells and two type III cells became type I cells. All these four alterations were single event transitions in SSTO activities indicating that the presence or absence of LTOs is a definitive characteristic of a given cell, whereas those of the SSTOs can appear and disappear in rare cases. In addition, when we made whole cell recordings in animals anesthetized with a mixture of midazolam, medetomidine, and fentanyl ($n = 21$; on top of the 61 reported above) instead of ketamine and xylazine, we observed the same consistent types of oscillations. Moreover, we did not find any evidence that the depth of ketamine–xylazine anesthesia affected the characteristics of the oscillations ($n = 8$; on top of the cells reported above) (SI Fig. 7*B*). In the latter recordings, the states and depths of anesthesia were determined with the use of electroencephalogram (EEG) recordings and qualified according to the frequency bands as described by Guedel (ref. 23; see also ref. 22), and we compared Guedel's stages III-2 and III-3 during recordings that lasted at least 40 min (SI Table 2).

Post hoc analysis revealed that properties such as resting membrane potential, membrane capacitance, firing rate, coefficient of variation for spike intervals, and the occurrence of rebound depolarizations and/or hyperpolarizing sags were all not significantly

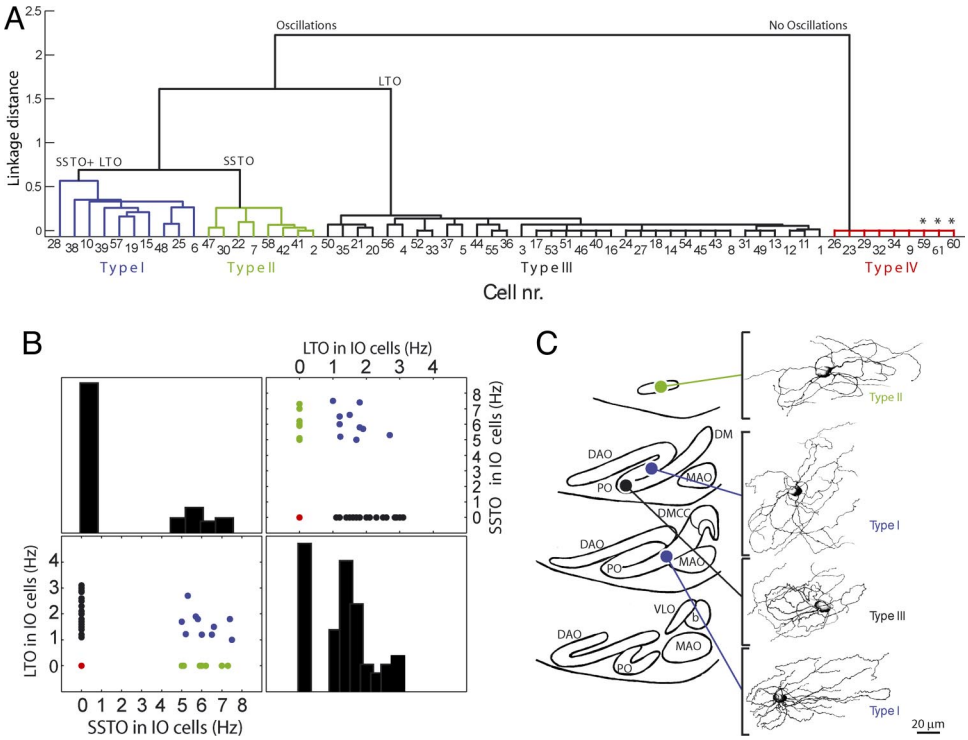


**Fig. 2.** Cluster analysis based on subthreshold oscillations in membrane potential. (*A*) Hierarchical cluster analysis shows clustering into four distinctive groups: type I neurons (blue) exhibit SSTOs and LTOs; type II neurons (green) express only pure SSTO; type III (black) neurons express only LTO; and type IV neurons (red) exhibit no subthreshold activity. *, Olivary neurons presumably from the dorsal cap of Kooy (21). (*B*) Matrix plot representation of the subthreshold oscillation frequencies of olivary neurons and their classification by hierarchical cluster analysis. (*C*) Reconstruction of neurobiotin-labeled neurons. All labeled cells (three cell types) were located in the IO and revealed similar morphology. DAO, dorsal accessory olive; PO, principal olive; DM, dorsomedial group of PO; MAO, medial accessory olive; DMCC, dorsomedial cell column; VLO, ventrolateral outgrowth; β, beta cell group.

different among the four cell types (SI Table 3). In contrast, the occurrence of H-current induced-depolarizing sags was significantly lower in type III neurons, whereas their shortest preferred interspike interval (ISI) was significantly longer (all $P$ values <0.02), and the mean input resistance was significantly higher in type IV neurons (for comparisons with type I, II and III neurons all $P$ values <0.03) (SI Table 3).

Thus, we conclude that olivary neurons can be divided into four types with specific frequency characteristics of their subthreshold oscillations and specific membrane and response properties that are all relatively stable over time.

**Preferred Spiking Patterns.** To find out whether subthreshold oscillations contribute to the firing behavior of olivary neurons, their spiking patterns were analyzed in relation to their subthreshold activities. Even though the firing frequencies among the four types were not significantly different, their patterns of preferred spiking varied (Fig. 4). Type I neurons had a dominant preferred spiking pattern with an ISI of 139 ± 8 ms ranging from 120 to 190 ms in agreement with the rhythm of SSTOs (Fig. 4*A*). In addition, type I cells had a second preferred spiking pattern with an average ISI of 629 ± 74 ms ranging from 454 to 802 ms corresponding with the presence of LTOs. Type II neurons showed preferred spiking patterns with an ISI ranging from 78 to 211 ms, which was again in accordance with the wavelength of their SSTOs (Fig. 4*B*). In type III neurons only spiking patterns with long ISIs were found ranging from 460 to 641 ms (Fig. 4*C*), which was also in line with the presence of LTOs; this preferred spiking pattern was significantly different from those of neurons in the other types (SI Table 3; ANOVA: $P < 0.01$; post hoc least significant difference test: $P < 0.01$). Finally, as expected from the subthreshold activities, type IV neurons showed no preferred spiking patterns (Fig. 4*D*). If one directly correlates the frequencies of preferred spiking with those of the subthreshold oscillations on a cell by cell basis, the correlation becomes evident ($r^2 = 0.95$) (Fig. 4*E*).

**Response Properties.** Somatosensory stimulation-evoked action potentials and excitatory postsynaptic potentials (EPSPs) in vast majority (85%) of the type I, II, and III neurons, but in none of the type IV neurons ($\chi^2$ test, $P < 0.05$; SI Table 2). The average response/stimulus efficiency was 23.6 ± 3.2% ($n = 20$) with an average response latency of 47.2 ± 3.9 ms ($n = 20$). Each cell type had a characteristic pattern of responding. In type I neurons stimuli evoked action potentials as well as EPSPs at short latencies of 37.1 ± 7.1 ms or long latency responses of 411 ± 113 ms (for mixture of short and long second latency responses, see Fig. 5*A*). In type II neurons the short latency responses were comparable with those in type I neurons, but the long latency responses (172 ± 23 ms) were significantly shorter ($P < 0.02$) (Fig. 5*B*). Moreover, in these neurons the stimuli did not only elicit action potentials or subthreshold potentials but they also reset the phase of the sinusoidal subthreshold oscillations; these resettings did occur both after the stimuli that evoked action potentials and after those that only evoked subthreshold potentials (Fig. 5 *B2* and *B3*). In type III neurons both the short latency responses (51.2 ± 5 ms) and long latency responses (516 ± 38 ms) were longer than those of type I and type II neurons ($P < 0.02$) (Fig. 5*C*). Moreover, the average inhibition period (465 ± 43 ms) that followed the stimulus-evoked responses was significantly longer in these cells ($P < 0.02$). In general, the length of these inhibition periods was longer when the stimulus evoked an action potential than when it only evoked an excitatory subthreshold response (compare Fig. 5 *B* and *C*). These results indicate a strong modulatory influence of peripheral inputs on olivary subthreshold oscillations and spiking patterns (i.e., olivary output).

**Interactions of Oscillations and Spiking Behavior.** The data provided above suggest that action potentials can reset the phase of the subsequent subthreshold oscillations in an accurate manner, which has also been observed *in vitro* (24). To further quantify this relationship, we compared the phase of the oscillations before and after the action potentials in type II neurons (Fig. 6). The phase of the subthreshold oscillations of type II neurons was only reset after the occurrence of spontaneous or stimulus-evoked action potentials when these action potentials did not occur exactly at the peak of the oscillation. The phase of their

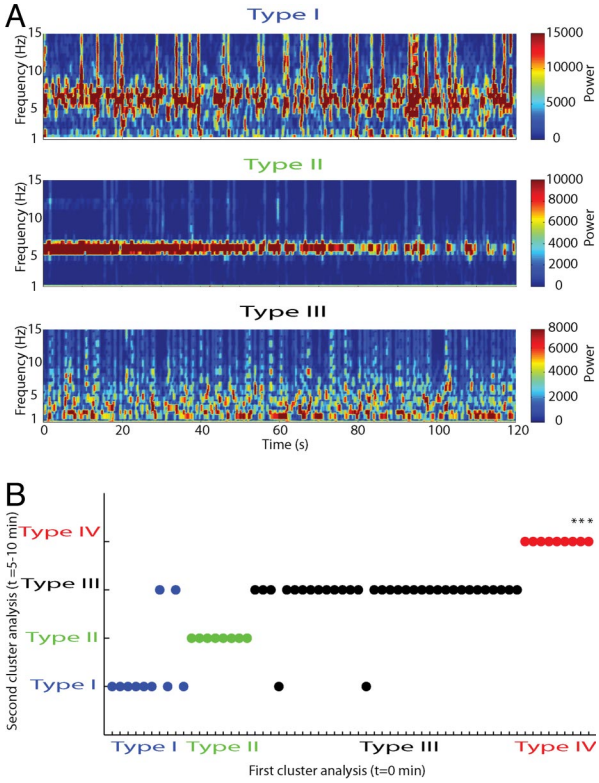


**Fig. 3.** Stability of subthreshold oscillation frequencies in olivary neurons. (*A*) Time-subthreshold oscillation frequency representation of 120 s of spontaneous recordings from a type I, type II, and type III neuron. The amplitude of the power spectra is coded in color. (*B*) Olivary neurons were subjected to two cluster analyses that were performed on oscillatory behavior that was obtained at two different time frames that were separated by 5–10 min. *, Olivary neurons presumably from the dorsal cap of Kooy (21).

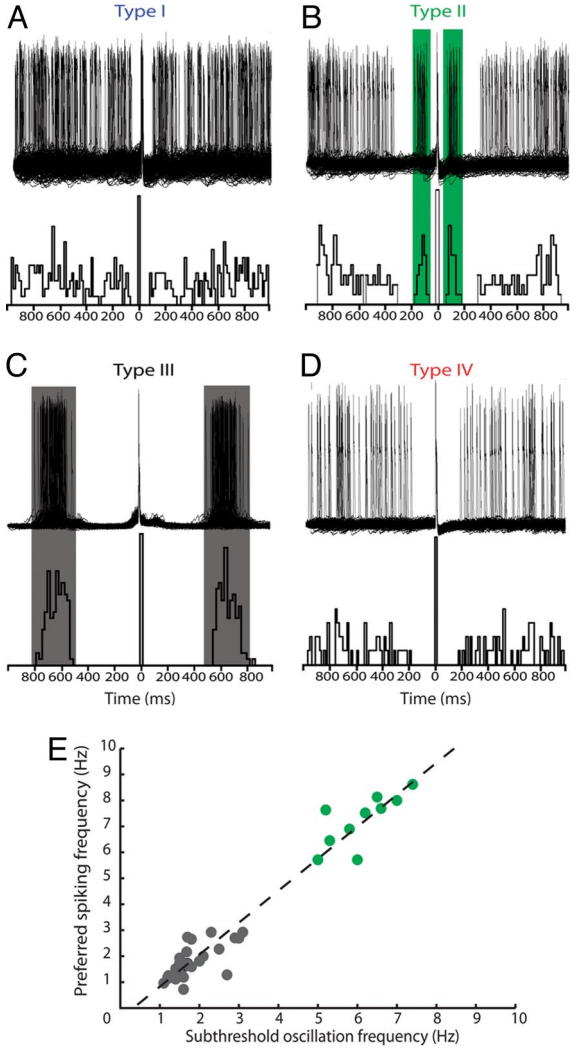


**Fig. 4.** Autocorrelograms showing preferred spiking patterns. (*A*) A type I neuron showing multiple preferred spiking patterns. (*B*) A type II neuron showing a preferred spiking pattern at 80–200 ms (indicated by green box). (*C*) Example of a type III neuron, which shows a preferred spiking pattern at 600–800 ms (indicated by gray box). (*D*) A type IV neuron showing no preferred spiking pattern. (*E*) Correlation between olivary oscillation frequency and preferred spiking pattern frequency (linear fit: $y = 1.2x - 0.4$; $r^2 = 0.95$).

oscillations after the action potential was consistently reset such that the new sinusoidal peaks occurred in cycles of ≈360° after the preceding action potential (Fig. 6). This relation held true for both spontaneous action potentials and stimulus-evoked action potentials, but the phase shift seemed to be somewhat greater after the stimulus-evoked potentials (Fig. 6).

The interaction between spiking behavior and subthreshold oscillations was not a one way interaction: The spiking behavior did not only influence the phase of the following oscillations, but the phase of the oscillation also strongly influenced the probability for an action potential to occur. Fig. 6 illustrates that there were virtually no cells spiking in the trough of the oscillation (between 180° and 360°). Thus, we can conclude that spiking behavior and subthreshold oscillatory behavior of olivary neurons strongly interact *in vivo*.

## Discussion

The present whole-cell recordings *in vivo* demonstrated that the vast majority of olivary neurons show subthreshold oscillations, that olivary neurons can be divided into four different categories dependent on the presence, shape and frequency of oscillation and that peripheral stimulation does not alter the characteristic stable oscillatory activities of an olivary cell other than resetting their phase. These findings have implications for the firing patterns of individual olivary neurons and they suggest that a wide variety of temporal patterns of olivary ensembles are composed by dynamically coupling or uncoupling specific types of olivary cells.

**Electrophysiological Composition of the IO.** The current *in vivo* study indicates that ≈85% of the inferior olivary neurons have spontaneous subthreshold oscillations. This finding suggests that the actual level of oscillations in intact mammals is higher than observed in *in vitro* studies, in which relatively few spontaneous oscillations occur and in which hyperpolarizing current injections or electrical stimulations are usually required to induce oscillatory activity (2, 6, 20). Possibly, the reverberating loops in which the IO is embedded enhance the intrinsic oscillatory properties of its neurons (25). These loops include the excitatory trajectories from the cerebellar nuclei and mesodiencephalic junction (26, 27) as well as the olivocerebellar modules comprising the olivary subnuclei, Purkinje cell zones and deep cerebellar nuclei (28). Such an extrinsic enhancing mechanism is in line with findings which indicate that serotonergic afferents to the olivary neurons as well as their level of electrotonic coupling can also modulate their propensity to oscillate (3, 29).

Apart from the nonoscillating cells, which presumably represent the neurons of the dorsal cap and ventrolateral outgrowth (21), we found three types of oscillating cells that could be identified based upon their spontaneous subthreshold activities and categorized accordingly using statistical cluster-analysis. They include type I

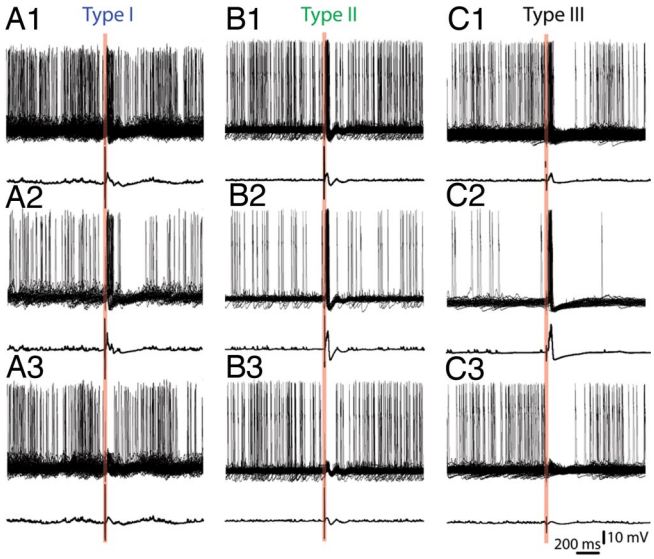


**Fig. 5.** Response properties after peripheral sensory stimulation. (*A1*) One hundred fifty traces of a type I neuron responding to peripheral stimulation and the resultant averaged trace indicated in the lower trace. (*A2*) Subpopulation of *A1*: the traces of the same neuron that responded with an action potential and their averaged trace indicated below. (*A3*) The complementary subpopulation of *A1*: the traces that did not respond with a spike and their averaged trace indicated below. (*B* and *C*) The same panels as in *A*, but for type II and type III cells. Note that the stimulus can induce a period of inhibition not only when it does induce an action potential (see *A2*, *B2*, and *C2*) but also when it does not (*A3*, *B3*, and *C3*). In *B3*, it can be seen that peripheral stimulation can even reset the phase of the oscillating subthreshold responses without action potentials. Red bars indicate the time of peripheral stimuli administration.

cells, which show both SSTOs and LTOs and which have a wide range of preferred frequencies for both their oscillations and spiking activities varying from 1 to 8 Hz; type II cells, which show only SSTOs and which have preferred oscillatory and spiking frequencies of 5 to 8 Hz; and type III cells, which show only LTOs and which oscillate and fire at preferred frequencies of 1 to 3 Hz. *In vitro* studies, in which the SSTOs and LTOs can be studied in isolation, have shown that these oscillations in the olive are generated by rhythmic activation of dendritic high-threshold and somatic low-threshold $Ca^{2+}$ conductances and their interaction with a $Ca^{2+}$-dependent $K^+$ conductance (3, 20). In addition, the H-current can also contribute to the olivary oscillations (20).

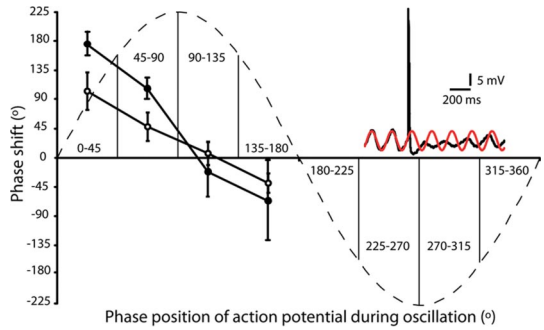


**Fig. 6.** Phase-response curves. The phase of the subthreshold oscillations of type II neurons was reset after the occurrence of spontaneous (open circles) or stimulus-evoked (filled circles) action potentials when these action potentials did not occur exactly at the peak of the oscillation. (*Inset*) Example of a comparison of the phase values of the subthreshold oscillations before and after the occurrence of an action potential. Red trace is a sinusoidal fit of the trace before the occurrence of the action potential followed by an extrapolation after the occurrence of the action potential.

H-current dependent depolarizing sags were frequently observed in all three main oscillating cell types, but our data show that this current does not necessarily need to be expressed in order for the oscillations to occur. Thus, whereas the basic membrane properties of all olivary neurons are rather similar (see SI Table 3), they can vary substantially in their type of subthreshold oscillations.

The different sorts of oscillations of the various cell types were reflected in the spiking patterns in that the preferred frequencies of the autocorrellograms of olivary spike activities corresponded to those obtained from the spectral analyses of the subthreshold oscillations. Likewise the temporal spiking patterns that occurred after peripheral stimulation also reflected the type of oscillatory cell they were recorded from and varied accordingly. Type II neurons (SSTO-only) responded with an action potential or an EPSP, type III neurons (LTO-only) responded with a low-threshold $Ca^{2+}$ spike with or without an action potential followed by a long afterhyperpolarization, and type I neurons revealed a mixed response. The main response properties (rate and latency) described here for the mouse IO were comparable with those found for the olive in the awake cat and rabbit (30, 31), except for type III neurons that responded with slightly longer latencies. In addition, peripheral stimulation had a clear effect on the phase of the subthreshold oscillations; it consistently reset the phase of its peak toward 90°. Thus, peripheral inputs to the olive can modify the temporal code of its neurons both in relative terms (firing frequency) and absolute terms (precise moment in time).

**Functional Implications.** Importantly, the subthreshold activity and thereby the identity of the cells seemed remarkably stable throughout the recordings. Virtually none of the recorded cells switched during the recordings from one category to the other even though many of them lasted longer than half an hour. We hardly ever observed the short episodic oscillatory behavior, which has been described by Chorev *et al*. (7). This difference might be due to differences in species used or in methodology such as the use of sharp electrode recordings instead of whole cell recordings. We cannot exclude the possibility that the state of the animal affects the oscillations (32), but the stability was so profound that even unphysiologically strong, electrical stimulation of the tongue was not sufficient to convert the identity characteristics of the olivary neurons. These data suggest that individual olivary neurons have a rather unique, preferred frequency of oscillation, which is relatively fixed. Such an organization raises the possibility that the overall temporal structure of an ensemble of coupled olivary neurons can in principle be manipulated by including or excluding cells with particular preferred frequencies to the ensemble. Thus, because the olivary neurons can be dynamically uncoupled by the cerebellar GABAergic terminals that are apposed to the spines that are coupled by dendrodendritic gap junctions in the olivary glomeruli (1, 4, 10, 33, 34), it may well be that this input also controls both the size of and the overall preferred frequency of the olivary ensembles. In this constellation the excitatory inputs could then deliver the firing frequency and the fine-tuning for the phase of the activity in absolute time.

## Materials and Methods

***In Vivo* Whole-Cell Recordings.** C57BL/6 mice were anesthetized with a mixture of ketamine and xylazine (65 and 10 mg/kg i.p.), or a mixture of medetomidine, midazolam, and fentanyl (0.5 mg/kg, 5 mg/kg, and 0.05 mg/kg i.p., respectively). The body temperature was maintained at 37°C with the use of an anal thermosensor and a heating pad (FHC, Bowdoinham, ME). To perform stable *in vivo* recordings, the mouse was placed in supine position and the head was fixed (35). Neck surgery was performed to expose the ventral surface of the medulla oblongata, and the dura was removed. Whole-cell recordings were performed with borosilicate pipettes (with filament; outer diameter 1.5 mm, inner diameter 1.2 mm; Hilgenberg, Malsfeld, Germany) filled with 4 mM NaCl, 3.48 mM

NEUROSCIENCE

$MgCl_2$, 9 mM KCl, 10 mM KOH, 120 mM K-gluconate, 10 mM Hepes, 17.5 mM sucrose, 4 mM $Na_2ATP$, and 0.4 mM $Na_3GTP$ with pH 7.2 and osmolality at 290–310 mOsm·kg$^{-1}$. To label the recorded neurons, 0.5% neurobiotin was added to the internal solution. Current clamp recordings were amplified with a Multiclamp 700A (Axon Instruments, Foster City, CA), filtered at 10 kHz and digitized at 20 kHz with a Digidata 1322A (Axon Instruments). Membrane potentials were corrected for an 8-mV junction potential. Peripheral stimulation was provided by electrical stimulation to the tongue or skin. The stimulation protocol consisted of short bipolar stimulations (2 ms, 1.25 mA). Analysis was performed by using Clampfit 9.0 software (Axon Instruments). All animal procedures were in accordance with the guidelines of the ethical committee of the Erasmus Medical Center.

**Morphology.** After labeling the cells with neurobiotin, mice were transcardially perfused with 4% paraformaldehyde in 0.1 M phosphate buffer (PB). The brainstem was removed and postfixed in perfusate and subsequently rinsed overnight at 4°C in 0.1 M PB, pH 7.4, containing 10% sucrose. The brainstem was embedded in 10% gelatin and 10% sucrose. Tissues were fixed in 10% formaldehyde and 30% sucrose solution at room temperature for 2 h. Serial sections of 40 $\mu$m were cut on a cryo-modified sliding microtome (SM2000R; Leica, Nussloch, Germany). Sections were incubated overnight at 4°C in avidin-biotin-peroxidase complex (Vector Laboratories, Burlingame, CA), rinsed, and incubated in DAB (75 mg/100 ml). The reaction was stopped after visual inspection by rinsing in PB. Neurobiotin-labeled cells were reconstructed by using Neurolucida software (Microbrightfield Europe, Magdeburg, Germany).

**Membrane Properties and Responses.** Data analysis was performed on neurons with resting membrane potentials negative to −45 mV, typical olivary spike waveforms, and spike amplitudes >60 mV. In each neuron, the following membrane properties were determined: resting membrane potential, input resistance, membrane capacitance, time-dependent inward rectification ($I_H$), rebound depolarizations, and after hyperpolarizations. Patterns of spontaneous firing were studied in recordings from membrane potentials of at least 2 min. The spontaneous firing rate was determined as the inverse of the mean of all spike intervals. The coefficient of variation (CV) of spike intervals was computed by dividing the standard deviation of the spike intervals by the mean of the spike intervals. Preferred spiking patterns were studied by autocorrelograms of spontaneous spiking patterns, and burst patterns were evaluated by using a burst analysis method (Clampfit 9.0 software; Axon Instruments). Burst patterns with a significant Poisson surprise value (>5) were selected, spike times of the spikes in this burst were averaged, and this value was taken as the center point of the preferred spiking period. Subthreshold oscillations were quantified by measuring the frequency and amplitude of the oscillations. Spontaneous membrane potential recordings of at least 2 min were analyzed by using a Hann windowed fast Fourier transformation to generate a power spectrum. The stability of subthreshold oscillations within a single recording was monitored by using a running Hann windowed fast Fourier transformation. Every 250 ms, a power spectrum was generated by analyzing the last 819.2 ms.

Membrane responses evoked by 150 peripheral sensory stimulations were analyzed. The response efficiency was determined by dividing the amount of evoked action potentials (i.e., action potentials in the 25- to 100-ms time window after the stimuli) by the amount of sensory stimuli. The response latency was calculated as the average time latency of these evoked action potentials after the peripheral stimuli. The occurrence of a preferred spiking period after the stimuli-induced action potential was determined by using again the burst analysis method. The average response latency of the spikes within this preferred spiking period was calculated.

To quantify the effect of action potentials on the subthreshold oscillation, the phase difference in subthreshold oscillation before and after action potential was determined. In spontaneous membrane potential and in stimuli-induced activity recordings, a sine-wave was fitted in the subthreshold oscillation before a spontaneous or evoked action potential. The fitted curve was extrapolated to the oscillations succeeding the action potential. Based on this curve-fit, the position of the spike and the phase shift were calculated.

**Statistics/Cluster Analysis.** Neurons were initially grouped by visual inspection of their subthreshold activity. Hierarchical cluster analysis was used to confirm the grouping produced by this visual inspection and to generate a more reliable classification of the different groups. Hierarchical cluster analysis was performed by using the frequencies of subthreshold oscillations as distinguishing variable. In this hierarchical clustering, we used standardized parameter values to compute the Euclidean distance between objects. The calculated linkage distance was used to define the cell clusters. To reveal cluster differences in basic membrane or stimulus response properties, statistical analyses were performed by using ANOVA or the $\chi^2$ tests, and post hoc analysis was performed by using the least significant difference test. All numerical values in the text refer to mean ± SEM.

We thank P. Bazzigaluppi for his technical support. This work was supported by ZorgOnderzoek Nederland Medische Wetenschappen VENI (M.T.G.D.J.), Nederlandse Organisatie voor Wetenschappelijk Onderzoek, ZorgOnderzoek Nederland Medische Wetenschappen, Neuro-Bsik (Senter), Sensopac (European Union), and Prinses Beatrix Fonds (C.I.D.Z.).

1. De Zeeuw CI, Simpson JI, Hoogenraad CC, Galjart N, Koekkoek SK, Ruigrok TJ (1998) *Trends Neurosci* 21:391–400.
2. Llinas R, Yarom Y (1981) *J Physiol (London)* 315:549–567.
3. Llinas R, Yarom Y (1986) *J Physiol (London)* 376:163–182.
4. Llinas R, Baker R, Sotelo C (1974) *J Neurophysiol* 37:560–571.
5. Benardo LS, Foster RE (1986) *Brain Res Bull* 17:773–784.
6. Llinas R, Yarom Y (1981) *J Physiol (London)* 315:569–584.
7. Chorev E, Yarom Y, Lampl I (2007) *J Neurosci* 27:5043–5052.
8. De Zeeuw CI, Wylie DR, DiGiorgi PL, Simpson JI (1994) *J Comp Neurol* 349:428–447.
9. Voogd J, Glickstein M (1998) *Trends Neurosci* 21:370–375.
10. De Zeeuw CI, Holstege JC, Ruigrok TJ, Voogd J (1989) *J Comp Neurol* 284:12–35.
11. Sasaki K, Bower JM, Llinas R (1989) *Eur J Neurosci* 1:572–586.
12. De Zeeuw CI, Lang EJ, Sugihara I, Ruigrok TJ, Eisenman LM, Mugnaini E, Llinas R (1996) *J Neurosci* 16:3412–3426.
13. Lang EJ (2002) *J Neurophysiol* 87:1993–2008.
14. Welsh JP, Lang EJ, Sugihara I, Llinas R (1995) *Nature* 374:453–457.
15. Lang EJ, Sugihara I, Llinas R (2006) *J Physiol (London)* 571:101–120.
16. De Zeeuw CI, Chorev E, Devor A, Manor Y, Van Der Giessen RS, De Jeu MT, Hoogenraad CC, Bijman J, Ruigrok TJ, French P, *et al*. (2003) *J Neurosci* 23:4700–4711.
17. Leznik E, Llinas R (2005) *J Neurophysiol* 94:2447–2456.
18. Long MA, Deans MR, Paul DL, Connors BW (2002) *J Neurosci* 22:10898–10905.
19. Yarom Y, Llinas R (1987) *J Neurosci* 7:1166–1177.
20. Bal T, McCormick DA (1997) *J Neurophysiol* 77:3145–3156.
21. Urbano FJ, Simpson JI, Llinas RR (2006) *Proc Natl Acad Sci USA* 103:16550–16555.
22. Friedberg MH, Lee SM, Ebner FF (1999) *J Neurophysiol* 81:2243–2252.
23. Guedel AE (1920) *Signs of Inhalational Anesthesia* (Macmillan, New York).
24. Leznik E, Makarenko V, Llinas R (2002) *J Neurosci* 22:2804–2815.
25. Kistler WM, De Zeeuw CI (2002) *Neural Comput* 14:2597–2626.
26. De Zeeuw CI, Holstege JC, Ruigrok TJ, Voogd J (1990) *Neuroscience* 34:645–655.
27. Ruigrok TJ, Voogd J (1995) *Eur J Neurosci* 7:679–693.
28. Voogd J, Bigaré, F (1980) *The Inferior Olivary Nucleus* (Raven, New York), pp 207–305.
29. Placantonakis DG, Schwarz C, Welsh JP (2000) *J Physiol (London)* 524:833–851.
30. Gellman R, Gibson AR, Houk JC (1985) *J Neurophysiol* 54:40–60.
31. Leonard CS, Simpson JI, Graf W (1988) *J Neurophysiol* 60:2073–2090.
32. Tso MM, Blatchford KL, Callado LF, McLaughlin DP, Stamford JA (2004) *Neurochem Int* 44:1–7.
33. Devor A (2002) *Cerebellum* 1:27–34.
34. Onodera S, Hicks TP (1995) *J Comp Neurol* 361:553–573.
35. Margrie TW, Brecht M, Sakmann B (2002) *Pflügers Arch* 444:491–498.